Influence of the Output Circuits in Piezoelectric Vibrational Harvesters

Rumyana Stoyanova, Dimo Kolev, Velimira Todorova
TU – Gabrovo
Gabrovo, Bulgaria
ruma_stoyanova@abv.bg, uplift7@mail.bg, vili@tugab.bg

***Abstract* — Determining the energy that can be obtained from energy harvesting devices is one of the important tasks in the process of their design, since the main difficulty is the relatively minute amount of energy that must be precisely estimated for a better evaluation of their capabilities. Therefore, the output circuit of these devices is an important factor in determining the output power.**

I. Introduction

The current human civilization is inseparably connected with the electrical power as it is used to supply power to all kinds of devices. As such the necessary volume of electrical power continuously increases as the human population and its needs swell. One of the methods for powering low consumption electrical device is to use the methods of Energy Harvesting (EH – also known as Power Harvesting or Energy Scavenging). An energy harvesting process is usually the extraction of electrical energy from some external source, which is not suitable for large scale power yield and then transforming and storing it for small, usually autonomous devices. The source of the extracted power is generally a background phenomenon which has not direct significance for, or its nature is somewhat parasitic in regards to the supplied system.

TABLE I. Energy Harvesting Sources [1]

Energy Source	Energy Density
Acoustic source	0,003 μW/cm^3, for 75 dB 0,96 μW/cm^3, for 100 dB
Temperature difference	10 μW/cm^3
Ambient radio frequencies	1 μW/cm^2
Daylight	100 mW/cm^2 (direct sun light) 100 W/cm^2 (artificial light in closed rooms)
Thermoelectric	60 W/cm^2
Vibrations (microgenerators)	4 W/cm^3 (human motion – Hz) 800 W/cm^3 (machines – kHz)
Vibrations (piezoelectric)	200 μW/cm^3
Air current	1 μW/cm^2
Keystrokes	50 J/N
Piezo crystals in shoes	330 μW/cm^2
Manual electric generator	30 W/kg

Some of these systems are used in self-power devices, e.g., the energy of the ocean waves utilized by oceanographic monitoring sensors to operate autonomously, as others are applied in portable electronics, where they can power or recharge mobile phones, specialized computers, radio communication equipment, etc.

All these devices ought to be robust enough to withstand prolonged exposure to hostile environments, and to have a wide range of dynamic sensitivity.

II. Main Part

A. Types of Popular Harvesting Methods

The classification of the various Energy harvesting (EH) devices can be composed by the type of their primary energy source. This energy can be from thermal, vibrational, light, or sound type. The determining parameters are usually the energy density of the source and the conversion efficiency and the energy density output of the harvesters. Table I compares different types of sources for energy harvesters, the sources being different types of environmental phenomena [1].

Depending of the power source, the harvesters differ in construction and mode of operation. Also, each type of harvester has different output signals – for example: in shape and strength of the output signal. On Fig. 1, a generalized block diagram of the energy conversion processes of different harvester types is presented.

Despite the different operational principles and distinct structures for the various types of harvesting devices, they usually consist of three parts: the first is the energy source from which the electrical power will be scavenged and the second is the harvesting mechanism: consists of the structure which converts the ambient energy into electrical energy.

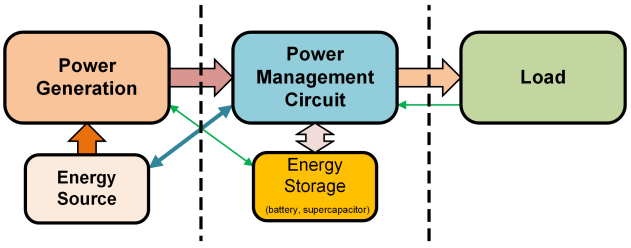

Fig. 1. General block diagram of EH devices

And the last is the load: actually, a device which consumes or stores the electrical output energy (Fig. 1).

The overall global goal regarding energy harvesting devices is to increase efficiency with more effective extraction technologies or, as the last resort, to utilize waste products from industrial and similar activities such as heat, vibration, noise, increased electromagnetic background and others [2, 3].

One of the more widely used methods of converting mechanical stresses into electrical energy is piezoelectric conversion. Piezoelectric EHs have certain advantages – such as a relatively high output voltage/mechanical voltage ratio; relatively easy methods for manufacturing the piezoelectric elements, etc. Due to the advantages of piezoelectric transducers, they are the subject of extensive research for mobile micro electrical autonomous sources [4].

B. *Piezoelectric Vibrational EH*

Vibrational piezoelectric EH systems have relatively the highest gain [5] without much dependence on external factors. Some harvesters are designed to collect the waste energy from human movement, as they are installed in a part of human clothing or accessories – for example, vibration harvesters are installed in the soles of shoes [6]. Other types are fixedly mounted in suitable locations so that passing vehicles [7, 8] or pedestrians exert a mechanical force on them.

The vibrating piezoelectric harvester can be considered as a generalized case of a beam structure with one or two anchored ends (shown on Fig. 2), described generally by the Euler-Bernoulli beam theory [7]. The parameters described in Fig. 3, are the length of the beam – L, the added mass at the tip – M_t, the resistance of the electric load – R_l.

The voltages on the resistive load for the cases of series and parallel connection respectively – $v_{ser}(t)$ and $v_{par}(t)$ [7].

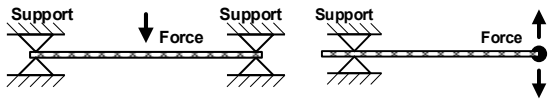

a) b)

Fig. 2. Usual mounting of vibrational piezoelectric EH

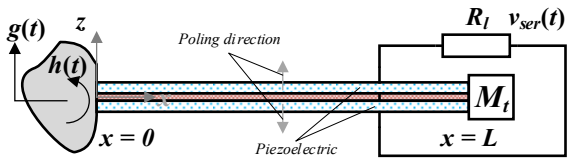

a) Serial connection

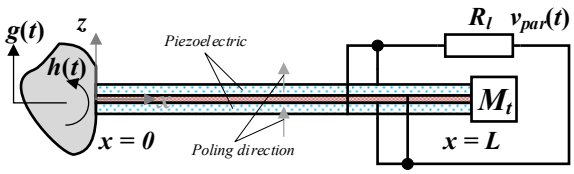

b) Parallel connection

Fig. 3. General diagram of EH device with two active layers [7]

That is due to the fact that the structure of EH (shown on Fig. 3) has two active (piezoelectric) layers that are connected to increase the current electrical density output of the piezoelectric EH system.

The piezoelectric beam system is usually assumed to be excited due to the movement of its foundation. Then, if the displacement and small rotation of the base are represented by $g(t)$ and $h(t)$, respectively, as shown on Fig. 3, the motion of the base $w_b(x, t)$ of the beam can be represented as [7], [9]:

$$w_b(x,t) = g(t) + xh(t) \tag{1}$$

The equivalent electromechanical equations governing the mechanical and voltage response of a bimorph can be given as [7]:

$$\frac{d^2\eta_r(t)}{dt^2} + 2\zeta_r\omega_r\frac{d\eta_r(t)}{dt} + \omega_r^2\eta_r(t) + \tilde{\theta}_r v(t) = f_r(t) \tag{2}$$

$$C_p^{eq}\frac{dv(t)}{dt} + \frac{v(t)}{R_l} = \sum_{r=1}^{\infty}\tilde{\theta}_r\frac{d\eta_r(t)}{dt} \tag{3}$$

where:
$\tilde{\theta}_r$ – modal electromechanical coupling term;
C_p^{eq} – the equivalent capacitance (depends on the connection between the layers);
$f_r(t)$ – modal mechanical forcing function;
$v(t)$ – voltage across the resistive load;
ζ_r – mechanical damping ratio;
$\eta_r(t)$ – mechanical modal response;
ω_r – undamped natural frequency of the r^{th} mode.

The right side of (3) is the expression that describes the electric current that can theoretically be obtained from the harvester. The describing models of piezoelectric harvesters usually represent the mechanical stresses that affect the structure through second-order partial differential equations, as shown in (2) [7], [9].

But the problem with the mathematical model based on the aforementioned equations for vibrating piezoelectric EH systems is that there are some equation constants and variables that depend on physical quantities that are indirectly or not at all related to the main variables that make up the general mathematical models – for example, the temperature in piezoelectric media is not directly included in the describing equations [7], [8].

C. *Piezoelectric vibrational EH Experimental Setting*

Experimental studies are carried out on a commercially available piezoelectric harvester [10] which will ensure that there is an assured degree of repeatability of the harvester parameters. The harvester is ***S233-H5FR-1107XB*** – bimorph structure with sequential connection of layers (previous designation *PPA-2014*). An electromechanical shaker with acceleration $a = 5{,}21$ m/s^2 is used to imitate the external mechanical stresses (Fig. 4a), and a functional generator is used to supply a harmonic signal through an amplifier to it (Fig. 4b).

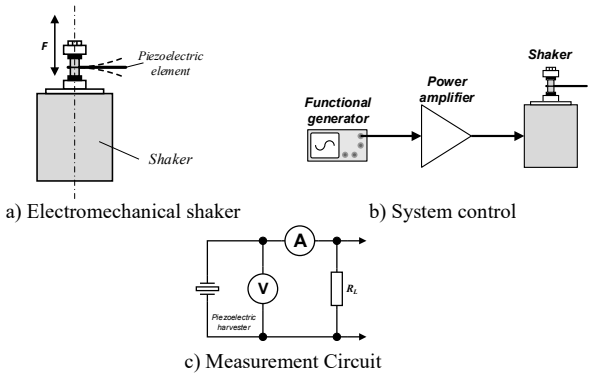

a) Electromechanical shaker b) System control

c) Measurement Circuit

Fig. 4. Basic experimental setup

The function generator is used to change the operating frequency while its output voltage is constant and has a value of *2* V peak-to-peak. Measurements are made with digital devices (DT9208A) that give the corresponding variable values in root mean square (RMS) form.

In fact, this form of data representation should be useful because for alternating electrical currents and voltages, RMS is equal to the value of the constant current or voltage that produces the same average power dissipation over a constant resistive load. Thus, the power that is measured in theory should be the actual active power that can be easily extracted and is the main goal of the harvesting process.

D. *Initial Experimental Result*

The first batch of experiments is carried out with an inertial mass of $m = 1{,}13\ g$ with different values for R_L and a single frequency of $f = 113\ Hz$. The initial voltage from the function generator was 2,65 V peak-to-peak. The voltage results were in the expected range however the current values were a bit odd because they exceeded the expected values (Table II).

The power values are accordingly calculated for the voltage (P_U), the current (P_I) and their product (P_{UI}) since the electrical load resistance is known (Table III).

TABLE II. INITIAL RESULTS

R_L, Ω	390	1000	2400	5100	10000	12400	24000	51000	75000	100000
U_{RMS}, V	1,302	1,457	1,872	2,37	3,18	3,47	4,34	5,15	5,47	5,58
I_{RMS}, mA	4	3,92	3,68	3,46	3,10	2,92	2,38	1,62	1,22	1,14

TABLE III. DATA FOR THE OBTAINED POWER

R_L, Ω	U_{RMS} [V]	I_{RMS} [mA]	P_U [mW]	P_I [mW]	P_{UI} [mW]
390	1,302	4	4,347	6,24	5,208
1000	1,457	3,92	2,123	15,366	5,711
2400	1,872	3,68	1,46	32,502	6,889
5100	2,37	3,46	1,101	61,055	8,2
10000	3,18	3,1	1,011	96,1	9,858
12400	3,47	2,92	0,971	105,727	10,132
24000	4,34	2,38	0,785	135,946	10,329
51000	5,15	1,62	0,52	133,844	8,343
75000	5,47	1,22	0,399	111,63	6,673
100000	5,58	1,14	0,311	129,96	6,361

The results for electrical power are so different that the suggestion of a faulty experimental setup is not far-fetched.

But there is another explanation: the indicated values are for reactive power that is present in the system and cannot be extracted at all. The frequency of the process is relatively low (113 Hz), but the piezoelectric element that generates the electrical oscillations has predominantly capacitive characteristics and its internal impedance can accordingly be replaced by its reactance in the equivalent circuits, as seen in (3) of C_p[64].

Thus, rectification of the electrical signal of the harvester is necessary for a correct assessment of the received energy, since the rectifier should eliminate the influence of the reactive energy. Therefore, the experimental circuit is extended with the addition of a full rectifier bridge.

E. *Experimental Circuit with Rectifier*

The full bridge rectifier and capacitive elements are added to the experimental circuit as shown in Fig. 5, since the diodes are of the **1N4148** type and the capacitive elements have the following values: $C_1 = 1\ \mu F$ and $C_2 = 10\ nF$.

The mechanical frequency is 115 Hz and the magnitude of the generator voltage is 2 V peak-to-peak. The experimental setup is divided into an AC part and a DC part, and the experimental circuits are for VA and AV type (Fig. 5). It is true that some energy will be lost in the rectifier bridge and in the capacitive elements, but only the usable part of the electrical energy will be dissipated on the constant electrical load R_L.

The resulting DC power is much less than that detected before the rectifier (Table IV), but there is also no sign of diode heating, which would indicate more consumption in the rectifier unit. But the calculated powers are not noticeably different from each other. Thus, it can be assumed that much of the detected unrectified energy is of the reactive type and is useless for harvesting purposes.

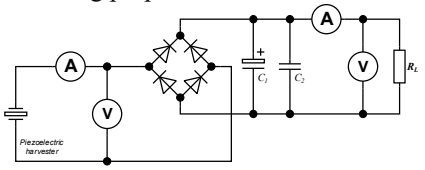

Fig. 5. Experimental setup with bridge rectifier

TABLE IV. EXPERIMENTS WITH RECTIFIER CIRCUIT

R_L, Ω	U_{RMS} [V]	I_{RMS} [mA]	P_U [mW]	P_I [mW]	P_{UI} [mW]	U_{DC} [V]	I_{DC} [mA]	P_{Udc} [mW]	P_{Idc} [mW]	P_{UIdc} [mW]
1000	1,3	2,9	1,69	8,41	3,77	0,2	0,245	0,04	0,060	0,049
2400	1,6	2,74	1,067	18,02	4,384	0,55	0,227	0,126	0,124	0,125
5100	1,99	2,56	0,776	33,42	5,094	0,99	0,208	0,192	0,221	0,206
7500	2,3	2,42	0,705	43,92	5,566	1,39	0,188	0,258	0,265	0,261
10000	2,58	2,3	0,666	52,90	5,934	1,74	0,174	0,303	0,303	0,303
12400	2,75	2,12	0,61	55,73	5,83	1,98	0,158	0,316	0,31	0,313
24000	3,38	1,72	0,476	71,00	5,814	2,9	0,122	0,35	0,357	0,354
51000	4,03	1,16	0,318	68,63	4,675	3,97	0,076	0,309	0,295	0,302
75000	4,26	0,9	0,242	60,75	3,834	4,5	0,055	0,27	0,227	0,248
100000	4,39	0,82	0,193	67,24	3,6	4,62	0,049	0,213	0,24	0,226

It can be speculated that a rectifier is ought to be included in the evaluation circuits for the piezoelectric harvesters as this is only reliable way to correctly asses the energy output. The results (shown on Fig. 6) for the power output after the rectifier are consistent with the expectations and there are no glaring differences between the calculated results. There is some difference in the calculated energies as shown on Fig. 6b when increasing the electrical load above the most efficient value (the value where the output energy is at its maximum) which can be attributed to some shift in the active and reactive parts of the electrical load.

The dependence between the obtained electrical energy and the equivalent capacitance as shown in (3) is theoretically also ought to lead to dependence between the overall capacitance of the output circuit and the volume of the obtainable energy.

F. Dependance between Output Energy and the Output Capacitance

Experiments are carried out to determine the connection between the output capacitance and the volume of the electrical energy. The mechanical stresses are the same as the changes are in the driving frequency and the connected capacitance in the output. The results for the 1 µF, 47 µF and 100 µF are respectively given in Table V, Table VI and Table VII.

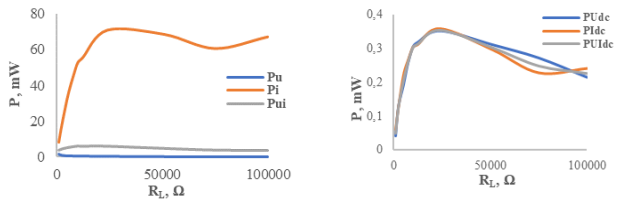

a) before the rectifier b) after the rectifier

Fig. 6. Results before and after the rectifier bridge

TABLE V. CAPACITANCE INFLUENCE FOR 1 UF

R_L, Ω	f, Hz	120	121	122	123	124	125	126	127
1000	P_{Udc}	0,281	0,250	0,240	0,240	0,240	0,314	0,423	0,336
	P_{Idc}	0,297	0,279	0,265	0,257	0,262	0,324	0,434	0,362
	P_{UIdc}	0,289	0,264	0,252	0,248	0,251	0,319	0,428	0,349
2400	P_{Udc}	0,651	0,651	0,630	0,600	0,641	0,900	1,053	0,900
	P_{Idc}	0,560	0,544	0,521	0,508	0,539	0,737	0,899	0,761
	P_{UIdc}	0,604	0,595	0,573	0,552	0,588	0,814	0,973	0,828
5100	P_{Udc}	0,865	0,832	0,816	0,832	0,865	1,559	1,367	1,177
	P_{Idc}	0,930	0,870	0,853	0,861	0,961	1,722	1,487	1,285
	P_{UIdc}	0,897	0,851	0,834	0,847	0,911	1,638	1,426	1,230
7500	P_{Udc}	1,145	1,114	1,137	1,479	2,059	2,285	2,101	1,835
	P_{Idc}	1,135	1,094	1,164	1,432	1,981	2,203	2,020	1,750
	P_{UIdc}	1,140	1,104	1,150	1,455	2,020	2,244	2,060	1,792
10k	P_{Udc}	1,204	1,170	1,218	1,332	1,781	1,697	2,247	1,927
	P_{Idc}	1,116	1,096	1,136	1,239	1,706	2,470	2,107	1,832
	P_{UIdc}	1,159	1,132	1,176	1,285	1,743	2,048	2,176	1,879
51k	P_{Udc}	1,142	1,097	1,160	1,283	1,660	2,607	2,266	2,020
	P_{Idc}	1,014	0,971	1,028	1,132	1,474	2,357	2,040	1,783
	P_{UIdc}	1,076	1,032	1,092	1,205	1,564	2,479	2,150	1,898
75k	P_{Udc}	0,950	0,883	0,952	1,082	1,374	2,140	1,972	1,736
	P_{Idc}	0,780	0,765	0,827	0,908	1,135	1,555	1,621	1,408
	P_{UIdc}	0,861	0,822	0,887	0,991	1,248	1,824	1,788	1,563
100k	P_{Udc}	0,814	0,792	0,835	0,918	1,313	1,814	1,615	1,423
	P_{Idc}	0,884	0,846	0,903	0,960	1,346	1,960	1,742	1,513
	P_{UIdc}	0,848	0,819	0,868	0,939	1,329	1,886	1,678	1,467

The obtained data confirm the assumption that the output capacitance has influence over the obtainable energy from the piezoelectric EH, as shown on Fig. 7. The comparison between the characteristics (Fig. 7) shows that there is difference between the most efficient frequency for energy harvesting depending on the connected output capacitance as well as there is a shift in the most suitable electrical load for maximum energy harvesting regarding the frequency of the mechanical stresses. These factors additionally complicate the designing of a general model of the vibrational piezoelectric EH with the aim for maximizing electrical energy output. The obtainable energy is in the range of several mW and every additional half milliwatt can make huge difference.

TABLE VI. CAPACITANCE INFLUENCE FOR 47 UF

R_L, Ω	f, Hz	120	121	122	123	124	125	126	127
1000	P_{Udc}	0,757	0,846	0,846	0,774	0,672	0,640	0,518	0,490
	P_{Idc}	0,941	1,040	1,040	0,960	0,878	0,799	0,706	0,618
	P_{UIdc}	0,844	0,938	0,938	0,862	0,768	0,715	0,605	0,550
2400	P_{Udc}	2,054	2,185	2,204	2,054	1,855	1,667	1,504	1,320
	P_{Idc}	1,918	2,103	2,148	2,036	1,796	1,594	1,434	1,268
	P_{UIdc}	1,985	2,143	2,176	2,045	1,825	1,630	1,469	1,294
5100	P_{Udc}	3,013	3,216	3,248	2,998	2,743	2,457	2,187	1,933
	P_{Idc}	3,338	3,642	3,667	3,429	3,119	2,793	2,499	2,208
	P_{UIdc}	3,171	3,422	3,451	3,206	2,925	2,620	2,338	2,066
7500	P_{Udc}	3,731	4,092	4,181	3,960	3,633	3,267	2,895	2,558
	P_{Idc}	3,910	4,264	4,355	4,140	3,813	3,437	3,053	2,709
	P_{UIdc}	3,819	4,177	4,267	4,049	3,722	3,351	2,973	2,632
10k	P_{Udc}	4,147	4,665	4,706	4,449	4,070	3,660	3,283	2,916
	P_{Idc}	4,238	4,733	4,747	4,516	4,186	3,733	3,352	2,970
	P_{UIdc}	4,192	4,699	4,727	4,482	4,128	3,697	3,318	2,943
51k	P_{Udc}	3,643	4,295	4,518	4,365	4,066	3,696	3,309	2,962
	P_{Idc}	3,528	4,348	4,468	4,142	3,970	3,581	3,213	2,865
	P_{UIdc}	3,585	4,322	4,493	4,252	4,018	3,638	3,260	2,913
75k	P_{Udc}	2,976	3,714	3,763	3,710	3,460	3,142	2,830	2,495
	P_{Idc}	2,940	3,630	3,730	3,663	3,435	3,030	2,736	2,484
	P_{UIdc}	2,958	3,672	3,746	3,686	3,448	3,085	2,783	2,490
100k	P_{Udc}	2,359	2,948	3,031	2,934	2,789	2,481	2,214	1,985
	P_{Idc}	2,890	3,534	3,725	3,423	3,349	3,028	2,723	2,403
	P_{UIdc}	2,611	3,228	3,360	3,169	3,056	2,741	2,455	2,184

TABLE VII. CAPACITANCE INFLUENCE FOR 100 UF

R_L, Ω	f, Hz	120	121	122	123	124	125	126	127
1000	P_{Udc}	0,624	0,656	0,723	0,723	0,689	0,656	0,578	0,518
	P_{Idc}	0,692	0,819	0,867	0,903	0,865	0,774	0,706	0,640
	P_{UIdc}	0,657	0,733	0,791	0,808	0,772	0,713	0,638	0,576
2400	P_{Udc}	1,700	1,855	2,128	2,166	2,091	1,962	1,768	1,568
	P_{Idc}	1,430	1,734	1,974	2,001	1,979	1,854	1,661	1,502
	P_{UIdc}	1,559	1,794	2,050	2,082	2,034	1,907	1,714	1,535
5100	P_{Udc}	2,569	2,952	3,264	3,377	3,106	2,906	2,861	2,569
	P_{Idc}	2,673	3,330	3,388	3,599	3,513	3,463	3,248	2,946
	P_{UIdc}	2,621	3,135	3,325	3,486	3,303	3,172	3,048	2,751
7500	P_{Udc}	3,162	3,536	4,166	4,424	4,048	3,975	3,661	3,360
	P_{Idc}	3,337	3,707	4,241	4,366	4,163	3,931	3,675	3,550
	P_{UIdc}	3,248	3,620	4,204	4,395	4,105	3,953	3,668	3,454
10k	P_{Udc}	3,226	3,624	4,199	4,665	4,733	4,489	3,944	3,844
	P_{Idc}	3,158	3,697	4,264	4,638	4,720	4,556	4,186	3,881
	P_{UIdc}	3,192	3,660	4,231	4,651	4,727	4,523	4,063	3,863
51k	P_{Udc}	2,141	2,133	2,521	2,795	2,777	2,730	2,593	2,364
	P_{Idc}	2,040	2,122	2,424	2,745	2,840	2,840	2,559	2,357
	P_{UIdc}	2,090	2,128	2,472	2,770	2,808	2,785	2,576	2,361
75k	P_{Udc}	1,404	1,667	1,882	2,080	2,113	2,067	2,004	1,706
	P_{Idc}	1,229	1,491	1,710	1,896	1,944	1,872	1,825	1,733
	P_{UIdc}	1,313	1,576	1,794	1,986	2,027	1,967	1,913	1,719
100k	P_{Udc}	1,121	1,362	1,545	1,713	1,695	1,656	1,563	1,364
	P_{Idc}	1,346	1,664	1,904	1,960	1,932	1,988	1,932	1,638
	P_{UIdc}	1,228	1,505	1,715	1,833	1,810	1,815	1,738	1,495

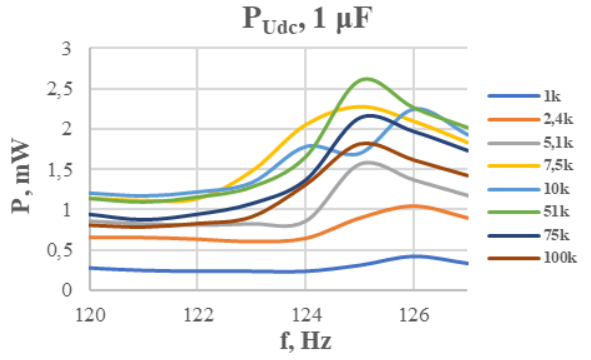

a) Results for 1 µF

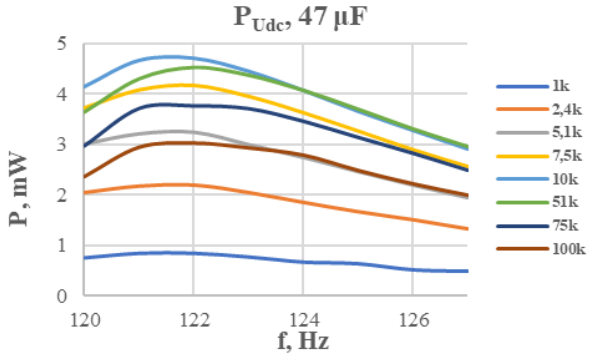

b) Results for 47 µF

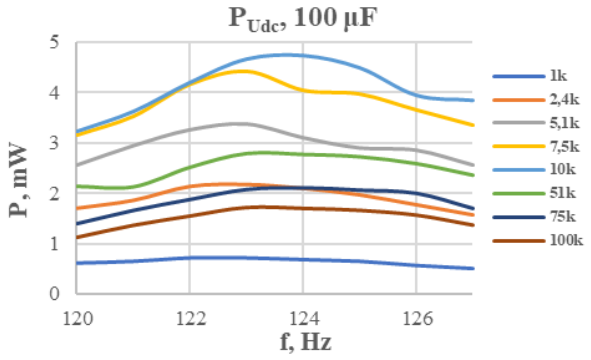

c) Results for 100 µF

Fig. 7. Results with different capacitances

It should be noted that in all of the experiments the used rectifier bridge is considered as ideal one. In Table VIII are given the results from the preliminary experiments with regards with the rectifier bridge. The experiments are done with VA-VA measurement circuit on 113 *Hz* frequency with inertial mass of 1,13 *g* as the alternating voltage and current values (U_{RMS} and I_{RMS}) are in RMS format.

TABLE VIII. PRELIMINARY RESULTS WITH RECTIFIER BRIDGE

Load, Ω	U_{RMS} [V]	I_{RMS} [mA]	P_U [mW]	P_I [mW]	P_{UI} [mW]	U_{DC} [V]	I_{DC} [mA]	P_U [mW]	P_I [mW]	P_{UI} [mW]
390	1,302	4	4,34668	6,24	5,208	0,171	0,343	0,07498	0,04588	0,05865
1000	1,457	3,92	2,12285	15,3664	5,71144	0,334	0,331	0,11156	0,10956	0,11055
2400	1,872	3,68	1,46016	32,5018	6,88896	0,791	0,301	0,2607	0,21744	0,23809
5100	2,37	3,46	1,10135	61,0552	8,2002	1,382	0,275	0,37449	0,38569	0,38005
10000	3,18	3,1	1,01124	96,1	9,858	2,34	0,232	0,54756	0,53824	0,54288
12400	3,47	2,92	0,97104	105,727	10,1324	2,69	0,214	0,58356	0,56787	0,57566
24000	4,34	2,38	0,78482	135,946	10,3292	3,89	0,162	0,6305	0,62986	0,63018
51000	5,15	1,62	0,52005	133,844	8,343	5,35	0,101	0,56123	0,52025	0,54035
75000	5,47	1,22	0,39895	111,63	6,6734	5,99	0,073	0,4784	0,39968	0,43727
100000	5,58	1,14	0,31136	129,96	6,3612	6,17	0,066	0,38069	0,4356	0,40722

The rectified values are respectively designated as U_{DC} and I_{DC} in Table VIII. The interesting part of the shown table is not that the alternating power calculated against the alternating voltage U_{RMS} is somewhat closest to the results from the rectified parameters but the fact that after the load resistance value is increased past the most efficient value (for obtaining the maximum electrical energy volume), the rectified voltage values become greater than the relevant values for the measured RMS voltage values (when the electrical load R_l is above 24 kΩ).

G. *Influence of the Bridge Rectifier*

The abovementioned effect can be assumed to be the result of a voltage multiplier circuit. That is in fact a diode-capacitor circuit that is created with the connection of the output capacitance and the rectifier bridge diodes. The diodes themselves have their own capacitance – the diffusion capacitance (C_D) when under direct bias and transition capacitance (C_T) when reverse biased. The transition capacitance depends on the value of the reverse bias voltage and the diffusion capacitance is directly proportional to the direct current through the diode and both capacitances can be represented as parallelly connected capacitor to the diode structure. The fact is the voltages over the bridge diodes are with "variable" magnitudes in the operational process of the piezoelectric harvester which additionally complicates the description of the circuit behaviour. Therefore, the both capacitances are not constant when the relevant biases are applied to the diodes but their values should vary accordingly to the signal magnitude and form from the piezoelectrical harvester and the frequency of the external mechanical stresses.

The nonlinearity of the diodes also plays its role as can be seen from Table VIII for the rectified voltages for the first three electrical loads (390 Ω, 1 kΩ and 2,4 kΩ). The alternating voltages for these loads can barely forwardly bias the diodes and the resulting power values are smaller from the rest.

The capacitances of the diodes and diode nonlinearity additionally decrease the available amount of harvestable electrical energy from the vibrational piezoelectrical EH. It is especially apparent when the voltages from the piezoelectric element are relatively small and comparable to the diode switch on voltages. Despite that the rectifier diode bridge is required for correct assessment of the available energy volume that can be harvested by the piezoelectric EH as the estimation through the alternating voltages and currents can lead to unintended bigger errors (Table III and Table VIII). The rectifier bridges are used in commercially available energy harvesting applications [11] (LTC3588) that are completely optimized for high output impedance energy sources such as piezoelectric transducers.

III. CONCLUSION

The amount of the available for harvesting electrical energy from EH devices is strongly connected with their inherent specifics as in the case of vibrational piezoelectric EH

the problem is their relatively low current density. But it is no such big matter when used to supply high impedance loads.

The bigger concern is the precise evaluation of the capabilities of the EH system which is also strongly connected with its output circuitry. The research for the most suitable output configuration concludes that there is necessity of rectifier circuit as the alternating values of the measurement circuit can lead to enormous error in estimating the harvestable power. The reason is the presence of the reactance power that is not at all usable for harvesting. The reactance part is due to default capacitance of the piezoelectric active element and the electrical load capacitance. The rectifier circuit will prevent the reactance power to be directed to the electrical load and therefore will allow to measure the real power output of the piezoelectric vibrational harvester.

Also, the research shows that the output capacitance can influence the volume of the obtainable energy which requires further study. The influence of the variable resistances and capacitances of the diodes from the rectifier bridge should decrease the obtainable energy but not drastically. The problem is to attune the piezoelectric harvester to operate in such frequencies that the received voltages are able to fully forward bias the diodes or the output capacitances can be picked up for maximum efficiency.

The output electrical loads should be selected in such matter that they ensure the maximum power output for the frequency range in which the vibrational piezoelectric harvesters operate.

ACKNOWLEDGMENT

The publication is funded under Project 2202C/2023, “Advanced engineering solutions for environmental management and protection- Stage II”.

REFERENCES

[1] F. Yildiz, *Potential Ambient Energy-Harvesting Sources and Techniques*, The Journal of Technology Studies, 2009, pp. 40-48, Published on 1 October 2009, DOI:10.21061/jots.v35i1.a.6.

[2] S. Zeadally, F. K. Shaikh, A. Talpur, Q. Z. Sheng, *Design architectures for energy harvesting in the Internet of Things*. Renewable and Sustainable Energy Reviews, 2020, 128, 109901, doi:10.1016/j.rser.2020.109901

[3] Inspire Clean Energy Blog, Web: https://www.inspirecleanenergy.com/blog/clean-energy-101/6-alternative-energy-sources

[4] S. Nurettin, K. Muammer, *Comprehensive review on the state-of-the-art of piezoelectric energy harvesting*. Nano energy, Vol. 80, February 2021, DOI: 10.1016/ j.nanoen.2020.105567.

[5] H. Wang, A. Jasim, X. Chen, *Energy Harvesting Technologies in Roadway and Bridge for Different Applications – A Comprehensive Review*. Applied Energy, Vol. 212 (2018), pp. 1083–1094, ISSN: 0306-2619.

[6] Ch. Sun, G. Shang, H. Wang, *On Piezoelectric Energy Harvesting from Human Motion*. Journal of Power and Energy Engineering, January 2019, 07 (01), pp. 155-164, DOI:10.4236/jpee.2019.71008.

[7] A. Erturk, *Electromechanical Modeling of Piezoelectric Energy Harvesters*, PhD dissertation thesis in Engineering Mechanics, Virginia Polytechnic Institute and State University, 20 November 2009.

[8] H. Xiong, *Piezoelectric Energy Harvesting for Public Roadways*. PhD dissertation thesis in Civil Engineering, Virginia Polytechnic Institute and State University, December 2014.

[9] M. F. Lumentut, I. M. Howard, *Electromechanical Finite Element Modeling for Dynamic Analysis of a Cantilevered Piezoelectric Energy Harvester with Tip Mass Offset under Base Excitations*. Smart Materials and Structures, 23(9), 2014, 095037, DOI:10.1088/0964-1726/23/9/095037.

[10] MIDE Technology, Web: https://piezo.com/collections/piezoelectric-energy-harvesters

[11] Analog Devices, Web: https://www.analog.com/en/products/ltc3588-1.html